

Surface structure of MgO (001): *Ab initio* versus shell model

Ye Li and David C. Langreth

Department of Physics and Astronomy, Rutgers University, P.O. Box 849, Piscataway, New Jersey 08855-0849

Mark R. Pederson

Complex System Theory Branch, Code 6691, Naval Research Laboratory, Washington, D.C. 20375-5345

(Received 25 May 1995; revised manuscript received 9 July 1996)

We have performed first-principles calculations on quasicubic MgO clusters for sizes up to 64 atoms. The results of these calculations have been used to determine a generalized environmentally dependent shell model (EDSM). In addition to reproducing the results from the first-principles calculations we suggest that the resulting EDSM parameters are more physical and more transferable than previous parametrizations based on bulk properties. First, we show that the force-constant matrix derived from the EDSM leads to an efficient approach to preconditioning. A full geometrical optimization of the quasicubic 64-atom MgO cluster is accomplished with a total of four first-principles force evaluations which is significantly less than what is required from a conjugate-gradient algorithm. Second, we use the shell-model parameters to study the relaxation and rumpling of an infinite (001) surface. The agreement between the EDSM and recent medium-energy scattering results is excellent and is significantly better than the agreement between conventional shell-model results and experiment. We show that these improvements are due to a more accurate accounting of the appropriate atomic polarizabilities: not only are these insensitively determined by previous methods, but also those for surface atoms are quite different from their counterparts for bulk atoms. [S0163-1829(97)00624-3]

I. INTRODUCTION

MgO is an ionic crystal with the NaCl structure. There exist a number of *ab initio* density functional calculations¹⁻⁴ of bulk MgO which successfully predict ground state properties such as lattice spacing. The (001) surface of MgO has an equal number of Mg and O atoms. This surface is the simplest and most stable, and forms without reconstruction. The properties of such a surface have been studied both theoretically⁵⁻¹⁸ and experimentally.¹⁹⁻³¹

This paper deals with the geometric structure of the surface. Madelung³² pointed out that the perpendicular displacement of the anions z_a and that of the cations z_c can be significantly different for an ionic crystal. The difference between the displacements $z_a - z_c$ is called the surface rumpling, while the mean movement of the surface layer $\frac{1}{2}(z_a + z_c)$ is called the surface relaxation. Normally both are expressed in percentages of the bulk nearest neighbor distance a . Rumpling is the result of the difference in the polarizabilities of the atomic species at the surface. The reason can be pictured as follows. As rigid ions, the Mg cations and the O anions experience the same Coulomb attraction from the bulk layers. The Mg cations are not polarizable, for the ten electrons are tightly bound by the $12e$ nuclear charge. The O anions are polarizable, for the outer electrons are more loosely bound to their nuclei. This difference in polarizability results in different nuclear movement for the two atomic species. One therefore expects the magnitude of surface rumpling to be very sensitive to the internal polarizabilities of the surface atomic species.

Knowledge of the geometric structure is a necessary prerequisite for the understanding of other properties. Consequently, the surface structure of MgO (001) has been studied extensively both experimentally and theoretically for more

than a decade. However, the conclusions have been controversial. Shell-model calculations,¹⁰⁻¹³ first-principles calculation within the Hartree-Fock (HF) approximation,¹⁴ a local density approximation (LDA) pseudo-potential calculation,¹⁵ a tight-binding calculation,¹⁶ dynamic low-energy electron diffraction (LEED) studies,²²⁻²⁵ and a reflection high-energy electron diffraction (RHEED) analysis²⁶ indicated a relaxation of no more than $\pm 3\%$ of the bulk atomic spacing. Despite all these consistent reports, an impact collision ion scattering spectroscopy (ICISS) study²⁷ reported a -15% (inward) relaxation. There has been even more debate over the magnitude of rumpling. To account for the anomalous enhancement of Kikuchi patterns of RHEED in their observations, Murata *et al.* reported 6% rumpling in the first layer for a UHV-cleaved surface when heated to 573 K and cooled down.²⁸⁻³⁰ Dynamic LEED studies of air-cleaved/vacuum-annealed surfaces by Welton-Cook and Berndt²³ reported only a 2% rumpling. Careful LEED studies of air-cleaved/vacuum-annealed, UHV-cleaved, UHV-cleaved/annealed surfaces by Urano *et al.* showed no rumpling regardless of surface preparation.²⁴ Recently, Blanchard *et al.* reported a rumpling of $(5 \pm 2.5)\%$.²⁵ The previously mentioned Hartree-Fock calculation¹⁴ predicted a rumpling of 1%, while the tight-binding calculation¹⁶ reported a first layer rumpling of 2.4% and the local density approximation (LDA) pseudopotential calculation¹⁵ gave a rumpling of 1.7%. Shell-model calculations gave more diverse values for surface rumpling. Welton-Cook and Prutton¹⁰ used four different inputs and found four different top layer rumplings ranging from -1.32% to 8.66%. Martin and Bilz¹¹ employed 12 different inputs and their results for the top layer rumpling varied from $-6-6\%$. The work by de Wette *et al.*¹² predicted a rumpling of about 2.4%.

In an effort to clarify the MgO (001) surface structure,

both experimental³¹ and theoretical investigations were initiated at Rutgers; preliminary joint work has appeared.³³ This paper will describe the results of our theoretical work, using both first-principles and shell-model approaches. We conducted *ab initio* calculations for a quasicubic cluster of 64 atoms. The equilibrium positions for this cluster was found. We introduce a generalized version of the classical shell model, the environmental dependent shell model (EDSM), to account for the different environments of the surfaces, edges, and corners. Its parameters were fitted to the *ab initio* results from the cluster. The structure for the infinite surface was solved with the resulting parameters for the EDSM. Our results are consistent with the most recent experimental results from medium-energy ion scattering.³¹

The basic assumption of our approach is that, although the forces on the various nuclei are somewhat different in the 64-atom cluster from what they are in a semi-infinite crystal, the polarizabilities and force constants that produce these forces are very local. This statement comes with the proviso that differing local environments are properly accounted for. An accomplishment of this work is to allow through the EDSM for different shell constants for different local environments, and to determine them *ab initio*. A still larger cluster would in addition allow us to account for the dependences of the shell parameters not only on local environment, but also on the environment of nearest neighbors, next-nearest neighbors, etc., a step that is deferred to subsequent work. Fortunately it is the common experience that in such highly ionic materials, the shell parameters do fall off rapidly with respect to range, so that the environmental dependence of the falloff becomes less important. In addition, we have several indirect consistency checks. The first deals with our worst case: our cluster has only eight atoms with bulk environments; the environments of the nearest neighbors of these bulk atoms in the cluster are not the same as for the semi-infinite crystal, there being too many nearest neighbors with surface environments. Nevertheless, as discussed in Sec. III B we get semiquantitatively correct results even for pure bulk properties. The effect of the bulk errors back on the surface properties should be even smaller. Such an expectation is confirmed by a previous all-electron calculation¹⁴ on this material, where it was found a substantial increase in the number of bulk atoms gave essentially no change in the prediction for the surface rumpling. Finally, we cite our previous work on MgO clusters,³⁴ which included studies of the effect of cluster size for clusters as large as 125 atoms.

In Sec. II we discuss the first-principles based methods used and introduce our EDSM. In Sec. III we use the EDSM as a technical aid in the *ab initio* geometrical optimization of the 64-atom cluster, reducing the number of *ab initio* force calculations to an order of magnitude less than would be needed using a standard conjugate-gradient method. The final EDSM parameters are then used to calculate the rumpling and relaxation of the infinite (001) surface. We also show physically what the important factors influencing the magnitude of the rumpling are and why previous shell-model calculations have obtained rather random predictions for this quantity. The values we obtained are in excellent agreement with the recent direct measurements by medium-energy ion scattering.³¹

II. METHOD

In this section, we describe the principles of our *ab initio* calculations and the details of the shell model. Since our *ab initio* method has been described elsewhere,³⁵ it will be presented very briefly. The shell model will be presented in detail.

A. First-principles calculations

The *ab initio* calculations are based on the Hohenberg-Kohn-Sham LDA (Ref. 36) with full electron potentials. We solve the Kohn-Sham equations,

$$\mathbf{h}\psi_i(\vec{r}) = \lambda_i\psi_i(\vec{r}), \quad (1)$$

self-consistently, where the Perdew-Zunger³⁷ expression for the exchange-correlation potential is used in the single particle Kohn-Sham Hamiltonian \mathbf{h} . The solution of (1) is achieved by expanding the single particle eigenfunctions $\psi_i(\vec{r})$ in a finite set of basis functions, diagonalizing the resulting matrix equation, and iterating to self-consistency. These basis functions include a linear combination of atomic orbitals (the radial parts of each expanded in a sum of Gaussians), plus a number of bare Gaussians times appropriate angular functions. From the self-consistent eigenfunctions the total energy E is evaluated as a function of nuclear position, using the Perdew-Zunger expression for the exchange-correlation energy.³⁷ The details of the calculational procedure can be found elsewhere.^{35,34}

The force on a nucleus at \vec{R}_ν may be calculated by numerically differentiating the energy curve

$$\vec{F}_\nu = -\frac{\partial E}{\partial \vec{R}_\nu}, \quad (2)$$

although we routinely calculate it directly through³⁸

$$\begin{aligned} \vec{F}_\nu = & -\int \frac{Z_\nu(\vec{R}_\nu - \vec{r})}{(\vec{R}_\nu - \vec{r})^3} \rho(\vec{r}) d\vec{r} + \sum_\mu' \frac{Z_\mu Z_\nu (\vec{R}_\nu - \vec{R}_\mu)}{|\vec{R}_\mu - \vec{R}_\nu|^3} \\ & - \sum_i \left[\int \frac{\partial \psi_i^*(\vec{r})}{\partial \vec{R}_\nu} [\mathbf{h} - \lambda_i] \psi_i(\vec{r}) d\vec{r} + \text{c.c.} \right], \quad (3) \end{aligned}$$

where Z_μ is the nuclear charge of the μ th nucleus, $\rho(\vec{r}) = \sum_i |\psi_i(\vec{r})|^2$, and the derivative $\partial \psi_i^*(\vec{r}) / \partial \vec{R}_\nu$ in the last summation indicates the derivative with respect to the explicit nuclear position dependence of the basis set.^{39,40} The inclusion of this last summation, which vanishes for an exact solution of (1), assures that (3) has the same variational accuracy as (2), when a finite local basis set is used. Throughout this paper, we will refer to forces calculated from (3) as the Hellman-Feynman forces, with the understanding that this last summation or Pulay correction⁴⁰ has been included.

B. Environmentally dependent shell model (EDSM)

Shell models have been widely used for equilibrium and dynamic properties of the bulk and surfaces of ionic crystals.^{10-13,41,42} The shell model we are going to describe has the same structure as model E in Sangster's work,⁴¹ but has been generalized so that its parameters can depend on the

TABLE I. Shell-model parameters.

A^{+-}	Twice the longitudinal force constant between Mg and O shell
B^{+-}	Twice the transverse force constant between Mg and O shell
A^{--}	Twice the longitudinal force constant between O shell and O shell
B^{--}	Twice the transverse force constant between O shell and O shell
Z	Absolute value of the Mg or O ionic charge
X	O-core charge
Y	O-shell charge, $X+Y=-Z$
a	Bulk atomic spacing between nearest neighbors
k	Spring constant between O shell and O core
G	Breathing constant of the O shell

local environment of the atom in question, in particular, whether it is a bulk atom, a surface atom, an edge atom, or a corner atom. A simple description of this model for MgO follows. In a MgO crystal, a magnesium atom loses about two electrons to the oxygen, so the remaining electrons are tightly bound. Therefore, a magnesium cation can be taken to move rigidly with no internal polarization. On the other hand, the outer electrons of an oxygen ion are loosely bound, and the electron clouds can be deformed by electric fields and mechanical compression. Less physically, the oxygen anion can be considered as a combination of a rigid core and a negatively charged shell. The interaction between the shell and the core is assumed to be harmonic and is characterized by a spring constant. The electrical and mechanical polarizabilities are mathematically related to the shell charge and the spring constant, so that the essence of the approximation is rather that the polarizabilities can be completely characterized by a small number of parameters. Intershell interactions are represented by longitudinal and transverse force constants. An oxygen atom interacts quantum mechanically with nearest neighbor magnesium atoms and next-nearest neighbor oxygen atoms. So we have O-Mg and O-O intershell interactions. Another important parameter is the shell breathing constant. Shell breathing, which will be discussed more later in this section, is unique for materials like MgO, which is not a perfectly ionic crystal. This shell model that we use is described in detail elsewhere;^{41,12} for convenience we list all the parameters with their definitions in Table I.

To make the definition of the first four parameters more specific, let $U_{\text{pair}}(|\vec{r}|)$ be the assumed exponential potential energy function for the relative motion between the pair of shells specified by the $+$ or $-$ superscripts, and let \vec{r}_{eq} be the equilibrium value of \vec{r} , so that $r_{\text{eq}}=a$ for nearest neighbors and $r_{\text{eq}}=\sqrt{2}a$ for second neighbors. Then, setting r_{\parallel} and r_{\perp} to be the components of \vec{r} parallel and perpendicular to \vec{r}_{eq} , respectively, we define

$$A = 2 \frac{\partial^2 U_{\text{pair}}(r)}{\partial r_{\parallel}^2} \Big|_{r=\vec{r}_{\text{eq}}} = 2 \frac{\partial^2 U_{\text{pair}}(r)}{\partial r^2} \Big|_{r=r_{\text{eq}}}, \quad (4)$$

and

$$B = 2 \frac{\partial^2 U_{\text{pair}}(r)}{\partial r_{\perp}^2} \Big|_{r=\vec{r}_{\text{eq}}} = 2 \frac{1}{r_{\text{eq}}} \frac{\partial U_{\text{pair}}(r)}{\partial r} \Big|_{r=r_{\text{eq}}}. \quad (5)$$

The number of independent shell-model constants in the list in Table I is 9, since $X+Y+Z=0$. However we use a to scale the units for the others. In particular, we take all the force constants A^{+-} , B^{+-} , A^{--} , B^{--} , and k to be measured in units of $e^2/2a^3$ and the various charges to be in units of e , so that neither a nor e will ever appear in the equations. The value for a is 3.98 a.u. or 2.106 Å. In addition, the static equilibrium condition requires that $\partial_a U_{\text{total}}=0$, thus giving the constraint³⁸

$$B^{+-} + 2B^{--} = -\frac{2}{3}\alpha_M Z^2, \quad (6)$$

where α_M is the Madelung constant $\alpha_M=1.7476$. Because of the a scaling and the above constraint, the number of degrees of freedom for the shell model is effectively only 7.

We define electrical and mechanical polarizabilities α and β , respectively, such that α is the unit cell dipole moment produced by a unit electric field and β is the distance the oxygen nucleus moves (relative to Mg) in response to the same unit field. We find that β is a more useful quantity in discussion of surface rumpling than the related mechanical polarizability d defined de Wette *et al.*¹² It will be useful to divide α and β into ‘‘rigid-ion’’ and ‘‘relaxation’’ pieces

$$\begin{aligned} \alpha &= \alpha^{\text{rgd}} + \alpha^{\text{rlx}}, \\ \beta &= \beta^{\text{rgd}} + \beta^{\text{rlx}}, \end{aligned} \quad (7)$$

where α^{rgd} and β^{rgd} are the contributions in the rigid-ion approximation in which the nucleus and its electrons are assumed to translate uniformly, and α^{rlx} and β^{rlx} account for the subsequent internal relaxation of the atomic electrons and nuclear position (in the shell model only the nucleus can relax). These quantities depend on frequency ω ; here we restrict ourselves to the cases $\omega=0$ and $\omega=\infty$, where the latter is taken to mean $\omega_{\text{phonon}} \ll \omega \ll E_{\text{gap}}/\hbar$; we label these two cases by subscripting the various quantities, e.g., α_0 , β_{∞} , $\beta_{\infty}^{\text{rlx}}$, etc. Within the shell model these polarizability components are given by

$$\begin{aligned} \alpha_0^{\text{rgd}} &= \frac{Z^2}{R}, & \alpha_0^{\text{rlx}} &= \frac{X^2}{k}, \\ \beta_0^{\text{rgd}} &= -\frac{Z}{R}, & \beta_0^{\text{rlx}} &= \frac{X}{k}, \\ \alpha_{\infty}^{\text{rgd}} &= \frac{Y(X+Y)}{R+k}, & \alpha_{\infty}^{\text{rlx}} &= -\frac{XY}{R+k}, \\ \beta_{\infty}^{\text{rgd}} &= \frac{Y}{R+k}, & \beta_{\infty}^{\text{rlx}} &= -\frac{Y}{R+k}. \end{aligned} \quad (8)$$

The quantity R in the above equations is dependent on local environment even within the traditional shell model. Specifically, for a bulk oxygen it is given by $R=A^{+-}+2B^{+-}$. For a surface oxygen it depends in addition on whether the displacement is perpendicular or parallel to the surface; in the former case one has $R=\frac{1}{2}A^{+-}+2B^{+-}$, while in the latter

$R = A^{+-} + \frac{3}{2}B^{+-}$. In our generalized EDSM, the quantities X , Y , and k also depend on local environment, and on displacement direction in the surface case.

The elastic constants, c_{11} , c_{12} , and c_{44} , which determine the long wavelength behavior of the bulk acoustic phonons, and the low and high frequency dielectric constants and frequencies of bulk optical phonons at long wavelength, are given below in terms of the bulk shell-model parameters. The elastic constants are³⁸

$$c_{11} = \frac{1}{2}(A^{+-} + A^{--} + B^{--}) - \gamma - (3C - \frac{1}{3}\alpha_M) Z^2, \quad (9)$$

$$c_{12} = \frac{1}{4}(A^{--} - 5B^{2-} - 2B^{+-}) - \gamma + (\frac{3}{2}C - \frac{5}{6}\alpha_M) Z^2, \quad (10)$$

$$c_{44} = \frac{1}{4}(2B^{+-} + A^{--} + 3B^{--}) + (\frac{3}{2}C - \frac{1}{6}\alpha_M) Z^2, \quad (11)$$

where C is the lattice sum $C = \sum_j' (q_i q_j / e^2) (a z_{ij}^4) / r_{ij}^5 = 1.0462$ and

$$\gamma = \frac{(A^{+-} + 2\sqrt{2}A^{--})^2}{2(G + 3A^{+-} + 12A^{--})}. \quad (12)$$

The frequency dependent dielectric constant ϵ_ω is given by

$$\epsilon_\omega = 1 + \frac{4\pi\alpha_\omega}{1 - (4\pi/3)\alpha_\omega}, \quad (13)$$

where α_ω is the polarizability of the bulk unit cell defined earlier, measured in units of the unit cell volume $2a^3$. Here we are only concerned with ϵ_0 and ϵ_∞ defined, respectively, for the low and high frequency limits defined earlier, denoted by $\omega=0$ and $\omega=\infty$ in Eq. (13). The zero wave vector longitudinal and transverse optical phonon frequencies ω_L and ω_T are given, respectively, by the frequencies at which ϵ_ω and ϵ_ω^{-1} vanish:

$$\omega_L^2 = \frac{\kappa}{\mu} \left[\frac{1 + (8\pi/3)\alpha_0}{1 + (8\pi/3)\alpha_\infty} \right], \quad (14)$$

and

$$\omega_T^2 = \frac{\kappa}{\mu} \left[\frac{1 - (4\pi/3)\alpha_0}{1 - (4\pi/3)\alpha_\infty} \right], \quad (15)$$

where $\kappa^{-1} = k^{-1} + R^{-1}$ and μ is the reduced mass of an Mg-O pair, the values of k and R to be used being the bulk ones. The ratio of Eq. (14) to (15) is just $\epsilon_0/\epsilon_\infty$ as required by the Lyddane-Sachs-Teller relation.

The shell breathing constant G is introduced for a material like MgO, which is not perfectly ionic. A simple shell model without shell breathing is one with an infinite G . With Eqs. (6), (10), and (11), it is easy to show that $c_{12} = c_{44}$ (Cauchy relation), if G is infinite, or in other words, if γ is zero. Indeed, in any central force model the Cauchy relation holds. For perfect ionic crystals like alkali halides, the Cauchy relation is well satisfied. However, the strong violation of the Cauchy relation for MgO implies some covalence and noncentral interaction. A shell model for MgO must introduce something new to simulate covalent interaction and hence to generate a noncentral force. Shell breathing increases the intraatomic energy of the oxygen atom, as well as affecting the intershell interaction. If the shell breathes by an

amount ΔR , the energy increases by an amount $\frac{1}{2}G\Delta R^2$, in addition to the energy change arising from the change in distance between the oxygen shell and neighboring ones. The above relationship defines G . The change of the interaction between the oxygen atom and a neighboring magnesium or oxygen is the same as if the oxygen atom were moved closer to its neighbor by an amount ΔR . A simple shell movement brings the shells closer to some neighboring atoms and further from some others. A shell breathing (expansion or contraction) brings the shell closer to or further from all its neighboring atoms by the same amount. This is how the noncentral force is generated in the shell model.

In traditional treatments, the parameters are usually all obtained by fitting bulk phonon dispersion curves. In the fitting process, one usually constrains the shell model to generate the elastic constants, the high and low frequency dielectric constants, and the transverse and longitudinal optical frequencies, which are the long wavelength (zero wave vector) phonon properties, and varies the remaining parameters to fit to the phonon frequencies at other wavelengths. The above procedure is equivalent to putting six more constraints on the fit. In other words, one has only one degree of freedom to vary in the fit to the bulk phonon frequencies at nonzero wave vector. A model as simple as this has been successful in obtaining reasonable fits. Nevertheless, as discussed in detail later, the parameters determined from bulk phonon fits do not work well for surface geometric structure.

III. CALCULATION AND RESULTS

Our theoretical work involved three steps. First, *ab initio* calculations were made on a finite neutral 64-atom cluster of MgO, and the equilibrium positions and force constants for small displacements from equilibrium determined. Second, the above data were used to determine the parameters of a generalized EDSM, which has been described in the previous section. Third, our generalized EDSM was solved for the structure of the infinite (001) surface. Such a procedure has the advantage of providing, in addition to the rumpling and relaxation of the planar surface in equilibrium, all the data necessary to determine in future work the surface phonon dispersions for this surface.⁴² It represents the first *ab initio* determination of the shell-model parameters that we are aware of.

A. *Ab initio* equilibrium positions for a 64-atom cluster

Here we present the results of calculations of the equilibrium positions of a 64-atom cluster, a $4 \times 4 \times 4$ quasicube with T_d symmetry. The equilibrium was found with the help of the shell model. We started with a configuration of the cluster in which the atomic spacings were 4.0 a.u. for all the nearest neighbors. We conducted a first-principles calculation on the cluster in this configuration and got the force on each atom. Then, we fitted the EDSM to these forces, allowing the parameter Y to vary from the values of Sangster depending on whether one was dealing with a bulk, surface, edge, or corner oxygen ion; the tensor character of k was accounted for by allowing it to take a different value for the displacement corresponding to each oxygen degree of freedom labeled 7–12 in Table II. The EDSM was used to calculate the force-constant matrix of the cluster, and new equi-

TABLE II. The force constants and equilibrium positions for the 12 independent degrees of freedom for nuclear motion (labeled by α). The force constants A_α and constrained equilibrium positions x_α^{ce} are related through the quadratic expression for the energy $E_\alpha(x_\alpha) = A_\alpha(x_\alpha - x_\alpha^{\text{ce}})^2 + C_\alpha$, where the x_α 's represent Cartesian components of an atom's nuclear position as indicated in column three of the table. The x_α^{ae} 's are the approximate equilibrium values of the x_α 's. The quantity x_α^{ce} is what the exact equilibrium value x_α for atom α would be if all the nuclear displacements corresponding to the other degrees of freedom were constrained to remain at their approximate equilibrium values. The origin is taken in the original center of the cluster. Atomic units $\hbar = m = e = 1$ are used.

α	Atom	Displacement	A_α	x_α^{ce}	x_α^{ae}
1	bulk Mg	(x_1, x_1, x_1)	1.208	1.939	1.931
2	surface Mg	$(x_2, -x_2, x_3^{\text{ae}})$	2.638	1.895	1.896
3	surface Mg	$(x_2^{\text{ae}}, -x_2^{\text{ae}}, x_3)$	0.713	5.897	5.888
4	edge Mg	$(x_4, x_5^{\text{ae}}, x_4)$	1.517	5.753	5.750
5	edge Mg	$(x_4^{\text{ae}}, x_5, x_4^{\text{ae}})$	1.520	1.944	1.930
6	corner Mg	$(x_6, -x_6, x_6)$	0.924	5.522	5.533
7	bulk O	$(x_7, -x_7, x_7)$	0.860	1.945	1.953
8	surface O	$(x_8, x_8, x_9^{\text{ae}})$	2.867	1.896	1.902
9	surface O	$(x_8^{\text{ae}}, x_8^{\text{ae}}, x_9)$	0.582	5.899	5.902
10	edge O	$(x_{10}, -x_{11}^{\text{ae}}, x_{10})$	1.221	5.818	5.844
11	edge O	$(x_{10}^{\text{ae}}, -x_{11}, x_{10}^{\text{ae}})$	1.607	1.881	1.869
12	corner O	(x_{12}, x_{12}, x_{12})	0.660	5.657	5.668

librium positions were predicted by using these force constants in conjunction with the Hellman-Feynman forces from the *ab initio* calculation. This process was repeated and after only four iterations, we got a configuration within which all the *ab initio* forces of the cluster were sufficiently small that the interatomic distances were estimated to be accurate to about 0.01 a.u. If more standard methods such as the conjugate gradient had been used to optimize the geometry, it would have taken a minimum of two calculations per degree of freedom and more probably five calculations per degree of freedom, for a total of minimally 24 and more probably 60 calculations. Our geometric optimization with just four calculations indicates the remarkable power of the EDSM method as a technical aid to *ab initio* minimizations. The equilibrium positions are illustrated in Fig. 1, and in a different notation in the final column of Table II, where they are labeled x_α^{ae} .

In our case we also needed to obtain accurate *ab initio* force constants in order to develop an *ab initio* fitted EDSM, discussed in Sec. III B below. To this end, the energies of 24 more configurations of the cluster were evaluated. In each configuration, one nucleus was moved a small distance (on the order of 0.04 a.u.) from its equilibrium position in a certain direction, with the equivalent nuclei moving equivalent amounts so as to keep the T_d symmetry. We had 12 independent degrees of freedom for the atomic displacements. For each degree of freedom, we made both a forward and a backward displacement. Therefore, for each degree of freedom, we had energies at three points, x_α^1 , x_α^2 , and x_α^{ae} , with the central point x_α^{ae} close to the minimum. Note this notation is meant to imply that the vector coordinate of a point is to be obtained by substituting one of the three values above for the x_α into the appropriate entry in the ‘‘displacement’’ column of Table II. By parabolic fit, we obtained the force constant A_α and the constrained equilibrium point x_α^{ce} for each degree of freedom. The above procedure is equivalent

to obtaining 12 force constants and 12 equilibrium points for 12 energy curves. The agreement between the (Pulay corrected) Hellman-Feynman forces and the forces obtained by differentiating the energy curves was carefully checked. The force constants and equilibrium positions x_α^{ce} are shown in Table II for each degree of freedom labeled by α .

We note that the point x_α^{ce} is what the equilibrium point for an independent displacement of degree of freedom α would be if all the other degrees of freedom were fixed at their original approximate equilibrium positions x_β^{ae} ($\beta \neq \alpha$); each force constant A_α is also the one appropriate for this constrained motion. Thus we have obtained the diagonal elements of the force matrix and not the whole matrix. Nevertheless the 24 pieces of diverse data (A_α and x_α^{ce}) comprise more than adequate information with which to fit the 18 free shell parameters, as described below in Sec. III B. The data on x_α^{ce} also verify that the accuracy of the approximate equilibrium distances (last column in Table II) is generally about 0.01 a.u.

Referring to Fig. 1, we see that for the relaxed 64-atom cluster the spacing between the inner Mg and O atoms is contracted. The spacing between the bulklike Mg and bulklike O is 3.88 a.u., which is about 2.5% smaller than the Mg-O spacing in the real bulk. This is a consequence of the surface stress which tends to round and contract a finite shape, an effect that prevents us from making a direct estimate of the relaxation of an infinite surface from the cluster results. However the calculation of the rumpling of the surfacelike atoms when calculated with respect to the bulklike atoms just below them does not suffer from this difficulty. The approximate equilibrium values in the last column of Table II give a surface-magnesium to bulk-oxygen spacing $x_3^{\text{ae}} - x_7^{\text{ae}} = 3.935$. This result is corrected by adding the amount $x_3^{\text{ce}} - x_3^{\text{ae}} = 0.009$ a.u., by which the magnesium atom

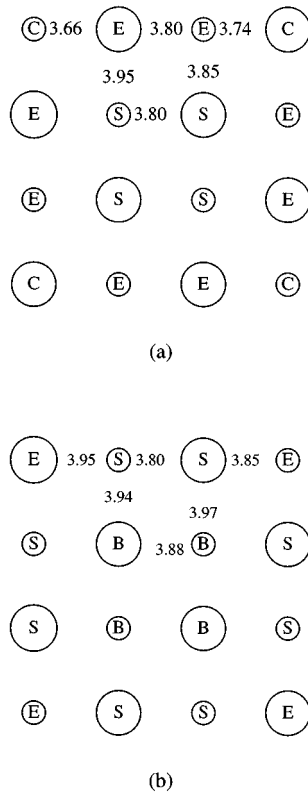


FIG. 1. The equilibrium positions of the 64-atom cluster. The larger circles represent O atoms, and the smaller circles represent Mg atoms. The plane shown in (a) is the surface, and the plane in (b) is the plane right below. The letters (*B,S,E,C*) in the figure represent bulk, surface, edge, and corner, respectively. The numbers between pairs of atoms are the calculated atomic spacings in a.u.

moves in finding its true constrained equilibrium position, for a resultant spacing of 3.944 a.u. Since the major part of the surface-magnesium atom's force constant comes from the oxygen atom directly below it, there should not be a significant change in this spacing from 3.944 a.u., when the rest of the cluster is allowed to relax. Likewise, it would be double counting to suppose that this spacing should be calculated as $x_3^{cc} - x_3^{ce}$. Repeating this little calculation for the surface-oxygen to bulk-magnesium spacing gives $x_9^{ac} - x_1^{ac} = 3.971$ for the initial estimate. This is corrected by adding $x_9^{ce} - x_9^{ac} = -0.003$ a.u., giving a resultant spacing of 3.968 a.u. The rumpling of the cluster is therefore $(3.968 - 3.944)/3.980 = 0.6\%$.

B. Shell-model fit

In this subsection, we will present our first-principles determination of the EDSM parameters. In the EDSM fit, different parameters were varied differently for physical reasons. The shell charge (equivalently the core charge) and spring constant were allowed to depend on the local environment, that is, they could take different values for the bulk, surface, edge and corner atoms. As we show in Sec. IIID the surface structure is very sensitive to β_0^{rlx} and α_0^{rlx} . Quantum mechanically we expect the polarizabilities of regions at the surface to be different from similar regions in the bulk, be-

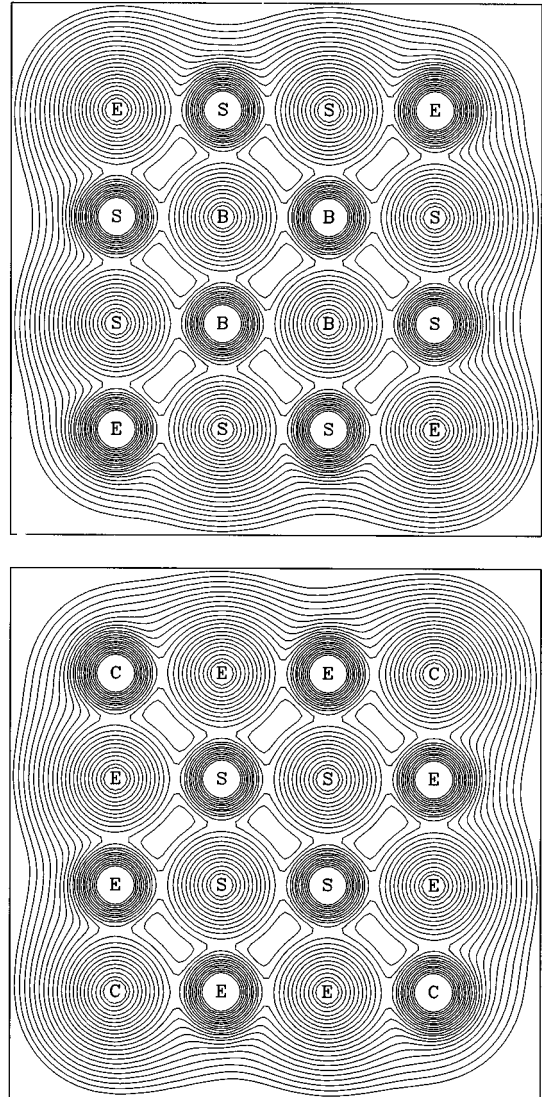


FIG. 2. The contour plots of the electronic density for the unrelaxed cubic 64-atom cluster. The atomic spacings are 4.0 a.u. The two plots, respectively, show the intersection of the equidensity surfaces with the surface atomic plane and with the atomic plane below it. Atomic sites are labeled with *B,S,E,C* for bulk, surface, edge, and corner atoms, respectively. The atoms with the larger sizes are oxygen atoms. The lowest density contour corresponds to a density of 0.001 a.u. and the density corresponding to each subsequent contour increases by a factor of $2^{1/2}$.

cause of the more diffuse wave functions and reduced gaps between occupied and unoccupied states that occur near the surface.^{1,5-8,19-21} Moreover the cubic symmetry is broken at the surface so that the polarizability's tensor nature must be accounted for. These expectations were translated to the shell model by allowing the parameters X , Y , and k to be dependent on local environment, and by taking the tensor nature of k into account. To avoid great complication, however, the nearest and second nearest neighbor parameters were not allowed to vary according to environment. These parameters are related to the overlap of real charge densities of the nearest and second nearest atoms. From the plots in Fig. 2 we see that the charge densities in the regions between the atoms are

not appreciably different in different environments. The shell breathing parameter, which was introduced to allow the Cauchy relation to be violated, was not varied in the fitting process. Given the tetrahedral deformations made on the cluster, the force constants obtained are unrelated to c_{44} . In other words, the force constants and equilibrium positions do not contain any information about the shell breathing constant G , so that the fit is insensitive to G . We tried several values of G and made a fit at each fixed value. We found that the results were not overly sensitive to a reasonable variation in G either. Therefore we simply adopted the choice $G=339.8$ as determined by Sangster⁴¹ in all our further work. So all in all there were 18 shell parameters obtained from the fit to the *ab initio* calculation: 6 k values for displacements 7–12 in Table II, four Z values and four Y values for each of the four environments (bulk, surface, edge, and corner), plus the two intershell force constants A and B for O-Mg interactions, and two for O-O interactions.

The objective of the EDSM fit is to reproduce the force constants and equilibrium points obtained from first principles. To do so, we used the shell model to calculate the energies of the same 25 configurations that had been calculated *ab initio* (see Sec. III A) and compared the two sets of results. By varying the shell-model parameters, we minimized the objective function

$$\sum_{\alpha=1}^{12} \sum_{i=1}^2 \{ [E_{\alpha}(x_{\alpha}^i) - E_0] - [E'_{\alpha}(x_{\alpha}^i) - E'_0] \}^2. \quad (16)$$

Here, as in the caption of Table II, $E_{\alpha}(x)$ is the energy of the configuration where the displacement from equilibrium corresponding to each degree of freedom (last column of Table II) is null except the α th, which has the argument x instead of x_{α}^{ae} . E_0 refers to the energy of the configuration where all atoms are at the positions implied by the 12 x_{α}^{ae} 's. The quantities x_{α}^1 and x_{α}^2 are the additional $2 \times 12 = 24$ points at which we made *ab initio* calculations. The unprimed E 's refer to the *ab initio* calculation, while the primed ones refer to the shell model.

The above procedure produced predictions for equilibrium position that were generally more accurate than 0.1% when compared with the *ab initio* ones; the surface to bulk distances crucial to the rumpling calculation were even accurate to 0.001 a.u. Similarly, the force constants were generally more accurate than 15% when compared with the *ab initio* ones, although the force constant for pushing a Mg edge atom towards the O corner had twice this error. The resulting EDSM parameters for the bulk and surface environments are tabulated in Table III. As part of our internal procedure, we also obtained shell constants Y and Z for the edge and corner environments, as well as values of k for each of the oxygen motion directions 7–12 in Table II and these are available elsewhere.⁴³

The bulk and surface polarizabilities are tabulated in Table IV. One sees that the full static bulk polarizabilities α_0 and β_0 are not much different from those of Sangster's model. However the much smaller internal or relaxation polarizabilities α_0^{rlx} and β_0^{rlx} sometimes differ from Sangster's by orders of magnitude. This shows simply that these much smaller polarizability components do not have much of an effect on the phonon frequencies, which according to Eqs.

TABLE III. Parameters obtained for our shell model. These are listed in the right three columns for the bulk and surface environments and displacement directions. A blank entry means that its value was constrained to equal that to its left. The parameters for Sangster's model are listed in column two; these do not vary with environment or displacement direction. Y and Z are in units of e , while the other quantities are in units of $e^2/2a^3$.

Parameter	Sangster	Bulk	Surface \perp	Surface \parallel
Z	1.92	1.74	1.73	
Y	-2.96	-1.76	-1.99	
X	1.04	0.018	0.266	
k	70.69	30.88	33.23	167.1
A^{+-}	30.81	27.07		
B^{+-}	-4.11	-3.77		
A^{2-}	0.288	-0.448		
B^{2-}	-0.088	0.143		
G	339.8	339.8		

(14) and (15) are sensitive only to the full α 's. Or by inversion one suspects that it is not possible to obtain reasonable values for the internal or relaxation polarizabilities by fits to bulk phonon spectra. This is compounded by the second important feature of Table IV, which is that the surface values of the static internal or relaxation polarizabilities differ by large factors from their bulk counterparts.

One may also use our EDSM to predict bulk properties. Bear in mind, however that there are only four oxygen ions in our cluster with bulklike environments, so that such predictions should be expected to be only qualitative. The seven bulk properties are shown compared with their experimental values in Table V. The agreement is generally satisfactory except possibly for ϵ_{∞} and ϵ_0 . The quantity actually determined directly in the latter case is α_0 , which according to Table IV is accurate to better than 15%. However the α_0 value is such that the denominator in Eq. (13) for ϵ_0 is small, so that errors in α_0 get magnified by a significant factor when calculating ϵ_0 . In the case of ϵ_{∞} , on the other hand, it is α_{∞} itself that differs from the experimental value by $\sim 35\%$. We suspect that this is due to a lack of variational freedom in the shell model itself: the nature of all distortions of the electronic charge cloud is parametrized by a single number, the shell charge Y . In the traditional shell models, α_{∞} is fitted directly to experimental data, typically at the cost of an implausibly large magnitude for Y , which leads to some of the static relaxation polarizabilities being in error by an order of magnitude or more. It is actually a tribute to the shell model that when fitted with a procedure such as ours which is sensitive to small components of the static polarizabilities, that the dynamic ones come out as *well* as they do. Finally, one should reiterate that the issue of c_{12} vs c_{44} has not been handled in an ideal fashion because of the inability of our tetrahedral cluster to reproduce shearing distortions.

C. Shell-model solution to the infinite surface

The procedure for the shell-model solution is fully described in the work by de Wette *et al.*¹² From their shell model, we reproduced their results for the MgO (001) surface with our ten-layer relaxation program, which was later

TABLE IV. Polarizabilities in the present work and in Sangster's model. The α 's are in units of $2a^3$ and the β 's are in units of $2a^3/e$. The blank entries for Sangster's model represent values that have been constrained by the model to be equal to the bulk entry to their left.

Quantity	Work	Bulk	Surface \perp	Surface \parallel
α_∞	Sangster	0.095	0.114	0.095
α_∞	present	0.063	0.136	0.028
α_0	Sangster	0.178	0.528	0.164
α_0	present	0.155	0.501	0.140
β_0	Sangster	0.070	0.253	0.063
β_0	present	0.088	0.281	0.079
$\alpha_0^{\text{rix}} \times 10^2$	Sangster	1.53		
$\alpha_0^{\text{rix}} \times 10^2$	present	10^{-3}	0.213	0.042
$\beta_0^{\text{rix}} \times 10^2$	Sangster	1.47		
$\beta_0^{\text{rix}} \times 10^2$	present	0.06	0.800	0.159

modified to include shell breathing. We then used our shell parameters from Table II to calculate the rumpling and relaxation, finding a rumpling of 0.5% with the surface-oxygen atoms outward relative the surface-magnesium atoms and an outward relaxation of 0.6% for the first layer. For the second layer, we found a rumpling of 0.1% and no relaxation. The main conclusion is that the relaxation and rumpling are very small and occur to a large degree only in the first layer.

D. How the surface polarizabilities affect rumpling

It is not surprising that the amount of rumpling is sensitive to the static electrical and mechanical polarizabilities. Here we give a more complete discussion of which components it is sensitive to and how this sensitivity arises.

As we discussed in Sec. IIB, these polarizabilities each have two components: a large rigid ion component and a much smaller component representing the internal or relaxation polarizability (see Table II). The important point to notice here is that the Madelung field from the bulk on a surface unit cell is not the uniform field for which the polarizabilities were defined, but is rather staggered, and thus provides little tendency for the rigid-ion motion of the cation relative to the anion. Said another way, the large rigid-ion components of the polarizabilities essentially cancel out of the rumpling problem, allowing the much smaller internal polarizabilities α_0^{rix} and β_0^{rix} to come to the fore.

To see how things go, let us suppose that, except for the single atomic layer at the surface, all atoms are held in their

TABLE V. Comparison among the phonon properties from our shell model and those from experiment. The unit for c_{11} , c_{12} , and c_{44} is 10^{12} dyn cm $^{-2}$, and the unit for ω_T and ω_L is 10^{13} cm $^{-1}$.

	Experiment	Present
c_{11}	2.89	2.85
c_{12}	0.88	0.66
c_{44}	1.55	1.16
ω_T	12.3	11.9
ω_L	22.0	21.2
ϵ_0	9.86	6.52
ϵ_∞	2.96	2.03

bulk positions and unpolarized internally. Let the electric field from these bulk ions at the position of a surface-oxygen ion be E_{bulk} . Then the outward movement of oxygen nucleus z^{rix} is given by

$$z^{\text{rix}} = \beta_0^{\text{rix}} E_{\text{bulk}}. \quad (17)$$

By actual calculation this internal relaxation component is the largest contributor to the rumpling in both our calculation and Sangster's model (0.8% and 2.2%, respectively), and Eq. (17) gives good rough estimates for these numbers.

The above does not however give the whole qualitative picture of what happens, because E_{bulk} also gives the oxygen ion an internal dipole moment p^{rix} given by

$$p^{\text{rix}} = \alpha_0^{\text{rix}} E_{\text{bulk}}, \quad (18)$$

which can interact with field gradients to produce rigid-ion motion. The principal effective field gradient at an O surface ion comes from the Mg ions in the surface layer. This gradient is 4–5 times stronger than the gradient of the Madelung field from the ions in the bulk, and favors an outward rigid-ion movement of the surface O ions. [Of course there is a field gradient of comparable magnitude from the surface O atoms, but the force it produces on another O dipole is exactly canceled by the force of their electric field on the other O monopole—said another way, the surface O atoms do not exert perpendicular forces on each other (by symmetry)]. If z is the perpendicular distance outward from the plane made by the surface magnesium ions, then for small z the field from the surface Mg takes the form $E = E'z$ along a line extending perpendicularly outward from an oxygen site, where E' is a constant. If the rigid-ion motion due to this field is dominant, then the force balance is between the inward direct interaction of the ionic charge $-Z$ with the field and the outward interaction of the induced dipole (18) with the field gradient. Thus we have $(-Z)E'z + E'p^{\text{rix}} = 0$, which gives upon substitution of Eq. (18)

$$z = \alpha_0^{\text{rix}} E_{\text{bulk}} / Z. \quad (19)$$

This gives a rigid-ion contribution to the rumpling which should be added to the relaxation contribution (17) above.

TABLE VI. Comparison of the relaxation and rumpling between various theoretical studies. Positive (negative) values of the relaxation refer to the expansion (contraction) between the first-layer and the second-layer atoms. Positive (negative) values of rumpling refer to outward (inward) displacement of the surface-O atoms with respect to the surface Mg atoms. Both quantities are in percentages of the bulk atomic spacing (2.106 Å).

Technique	Author(s)	Relaxation	Rumpling
Shell model	Welton-Cook and Prutton (Ref. 10)	0–0.9 %	–1.32–8.66 %
	Martin and Bilz (Ref. 11)	0–3%	–6–6 %
	Lewis and Catlow (Ref. 13)	–0.7%	11%
	de Wette <i>et al.</i> (Ref. 12)	–0.6%	2.4%
	Present work (Sangster) ^a	0.4%	3.8%
	Present work ^b	0.6%	0.5%
Tight binding	LaFemina and Duke (Ref. 16)	–1.4%	2.4%
LDA pseudopotential	Pugh and Gillan (Ref. 15)	0.7%	1.7%
Hartree Fock	Causa <i>et al.</i> (Ref. 14)	0%	0.9%
LDA full potential	Present work ^c (LDA)		0.6%

^aUsing Sangster’s shell-model E.

^bUsing our shell model with parameters fitted to *ab initio* calculation.

^c*Ab initio* calculations on the 64-atom cluster.

For Sangster’s model the exact rigid-ion contribution was calculated to be 1.6%, which is much too large because α_0^{rx} is much too large in that model. For our EDSM, the rigid-ion contribution was –0.3%; in this case α_0^{rx} was very small, so this mechanism (19) was not the operative one.

IV. DISCUSSION

Results from our theoretical work indicate very small relaxation and rumpling. This is in good agreement with the recent measurements of Zhou *et al.*,³¹ who also find very small deviations from a bulk truncated surface [a rumpling of $(0.5 \pm 1.0)\%$ and relaxation of $(-1.0 \pm 1.0)\%$]. A discussion of other relevant experimental work^{19–30} has been recently given by Zhou *et al.*³¹ With respect to theory, our results, together with those of others, are tabulated in Table VI for comparison. Generally the *ab initio* theoretical calculations predict rumplings and relaxations that are reasonably small.

The various shell-model calculations have on the other hand produced what appear to be random numbers for the rumpling and relaxation. In retrospect this is just what one would expect. Except for our EDSM, the shell-model parameters were fitted to bulk properties which were sensitive mainly to the total polarizabilities, and not to the internal or relaxation polarizabilities, which are tiny fractions of the total. Furthermore, even if a shell fit happened to get a roughly correct value for one of these small polarizabilities, it would be the polarizability of a bulk atom. As we have seen, the internal polarizabilities of the surface atoms, which are the controlling factors in the size of the rumpling, are quite different from those of the bulk atoms. Our EDSM circumvented these difficulties by (i) introducing shell parameters that depended on local environment and displacement direction and (ii) fitting directly to individual nuclear movements.

The method should be widely applicable to all environments involving combinations of bulk, surface, edges, and corners, and should be useful in discussing steps and kinks on surfaces. A slight generalization to include the environment of a single-layer step edge would probably be useful

here, as this may be sufficiently different from the edge environment modeled here to warrant the extra complexity. This would involve a repeating the calculations and fittings on a larger cluster. This would be desirable in any case to increase the number of bulk atoms and thus to improve the accuracy of the bulk parameters. Armed with this apparatus one should be able to tackle a wide variety of surface structural problems which involve combinations of these environments, and thus to transfer the simplicity of the shell model to situations that are difficult to study using *ab initio* methods. Of course, one could not hope that environments that are completely different, for example, the presence of an adsorbed metal atom, could be described without additional *ab initio* calculation. We suspect that even in this case, however, our model might be useful in obtaining the self-consistent positions of the substrate atoms not in immediate contact. The model should also be useful for surface vibrational structure calculations of the type performed in Ref. 42 using the simple shell model.

V. CONCLUSION

We conducted *ab initio* calculations on quasicubic clusters of 64 atoms with {001} faces. We obtained a rumpling of 0.6% for the surface O and Mg atoms on those faces with environments like those which these atoms would have on the semi-infinite (001) surface. A generalized shell model (EDSM) was fitted to the first-principles results. The model was then solved for the semi-infinite surface, giving a surface relaxation of 0.6% and a surface rumpling of 0.5% with the surface-oxygen atoms moving outward with respect to surface-magnesium atoms. These are consistent with other *ab initio* calculations predicting small values for these quantities (see Table VI) and also the recent studies³¹ by medium-energy ion scattering, which also gave small rumpling and relaxation.

We have introduced the EDSM by generalizing the traditional shell model to include effects of local environment, and have come to some understanding of the strengths and

weaknesses of these models. We showed why the traditional shell-model approach of fitting bulk properties has had but random success in predicting surface structural parameters. We have also invented a different technical use of the shell model as a tool in performing *ab initio* calculations, which allowed the equilibrium positions of the atoms in a large cluster to be determined *ab initio* with just three or four repetitions of the *ab initio* calculation.

ACKNOWLEDGMENTS

We thank M. Mehl and K. Jackson for discussions during the early stages of this work. Work supported in part by the National Science Foundation Grant Nos. DMR 89-07553, DMR 91-03466, and DMR 94-07055. Computer resources were provided in part by the Pittsburgh Supercomputing Center.

-
- ¹C. Li, R. Wu, A. J. Freeman, and C. L. Fu, *Phys. Rev. B* **48**, 8317 (1993).
- ²M. J. Mehl, R. E. Cohen, and H. Krakauer, *J. Geophys. Res.* **93**, 8009 (1988).
- ³K. J. Chang and M. L. Cohen, *Phys. Rev. B* **30**, 4774 (1984).
- ⁴Q. S. Wang and N. A. W. Holzwarth, *Phys. Rev. B* **41**, 3211 (1990).
- ⁵V. C. Lee and H. S. Wong, *J. Phys. Soc. Jpn.* **45**, 895 (1978).
- ⁶C. Satoko, M. Tsukada, and H. Adachi, *J. Phys. Soc. Jpn.* **45**, 1333 (1978).
- ⁷M. Tsukada, H. Adachi, and C. Satoko, *Prog. Surf. Sci.* **14**, 113 (1983).
- ⁸S. Russo and C. Noguera, *Surf. Sci.* **262**, 245 (1992).
- ⁹A. Gibson and R. Haydock, *J. Vac. Sci. Technol. A* **10**, 2361 (1992).
- ¹⁰M. R. Welton-Cook and M. Prutton, *Surf. Sci.* **74**, 276 (1978).
- ¹¹A. J. Martin and H. Bilz, *Phys. Rev. B* **19**, 6593 (1979).
- ¹²F. W. de Wette, W. Kress, and U. Schröder, *Phys. Rev. B* **32**, 4143 (1985).
- ¹³G. V. Lewis and C. R. A. Catlow, *J. Phys. C* **18**, 1149 (1985).
- ¹⁴M. Causà, R. Dovesi, C. Pisani, and C. Roetti, *Surf. Sci.* **175**, 551 (1986).
- ¹⁵S. Pugh and M. J. Gillan, *Surf. Sci.* **320**, 331 (1994).
- ¹⁶J. P. LaFemina and C. B. Duke, *J. Vac. Technol. A* **9**, 1847 (1991).
- ¹⁷J. Goniakowski and C. Noguera, *Surf. Sci.* **323**, 129 (1995).
- ¹⁸W. Langel and M. Parrinello, *Phys. Rev. Lett.* **73**, 504 (1994).
- ¹⁹V. E. Henrich, G. Dresselhaus, and H. J. Zeiger, *Phys. Rev. B* **22**, 4764 (1980).
- ²⁰P. R. Underhill and T. E. Gallon, *Solid State Commun.* **43**, 9 (1982).
- ²¹P. A. Cox and A. A. Williams, *Surf. Sci.* **175**, L782 (1986).
- ²²C. G. Kinniburgh, *J. Phys. C* **8**, 2382 (1975).
- ²³M. R. Welton-Cook and W. Berndt, *J. Phys. C* **15**, 5691 (1982).
- ²⁴T. Urano, T. Kanaji, and M. Kaburagi, *Surf. Sci.* **134**, 109 (1983).
- ²⁵D. L. Blanchard, D. L. Lessor, J. P. LaFemina, D. R. Baer, W. K. Ford, and T. Guo, *J. Vac. Sci. Technol. A* **9**, 1814 (1991).
- ²⁶P. A. Maksym, *Surf. Sci.* **149**, 157 (1985).
- ²⁷H. Nakamatsu, A. Sudo, and S. Kawai, *Surf. Sci.* **194**, 265 (1988).
- ²⁸Y. Murata, S. Murakami, H. Namba, T. Gotoh, and K. Kinoshita, in *Proceedings of the 7th International Vacuum Congress and the Third International Conference on Solid Surfaces*, edited by R. Dobrozemsky *et al.* (Berger & Söhne, Vienna, 1977), p. 2439.
- ²⁹T. Gotoh, S. Murakami, K. Kinoshita, and Y. Murata, *J. Phys. Soc. Jpn.* **50**, 2063 (1981).
- ³⁰Y. Murata, *J. Phys. Soc. Jpn.* **51**, 1932 (1982).
- ³¹J. B. Zhou, H. C. Lu, T. Gustafsson, and P. Häberle, *Surf. Sci.* **302**, 350 (1994).
- ³²E. Madelung, *Phys. Z.* **20**, 494 (1919).
- ³³J. B. Zhou, Y. Li, H. C. Lu, D. C. Langreth, and T. Gustafsson, P. Häberle, and M. R. Pederson, in *The Structure of Surfaces IV*, edited by X. D. Xie, S. Y. Tong, and M. A. van Hove (World Scientific, Singapore, 1994), p. 599.
- ³⁴Y. Li, D. C. Langreth, and M. R. Pederson, *Phys. Rev. B* **52**, 6067 (1995).
- ³⁵M. R. Pederson and K. A. Jackson, *Phys. Rev. B* **41**, 7453 (1990).
- ³⁶P. Hohenberg and W. Kohn, *Phys. Rev.* **136**, B864 (1964); W. Kohn and L. J. Sham, *ibid.* **140**, A1133 (1965).
- ³⁷J. P. Perdew and A. Zunger, *Phys. Rev. B* **23**, 5048 (1981).
- ³⁸Equations referring to *ab initio* calculations, such as those in Sec. II A, are expressed in atomic units $\hbar = m = e = 1$. Equations referring to shell-model quantities, such as those in Sec. II B are expressed in the following units: charges in units of e , shell force constants in units of $e^2/2a^3$ where a is the nearest neighbor spacing, electrical polarizabilities in units of $2a^3$, mechanical polarizabilities in units of $2a^3/e$, and elastic constants in units of $e^2/2a^4$.
- ³⁹K. Jackson and M. R. Pederson, *Phys. Rev. B* **42**, 3276 (1990).
- ⁴⁰P. Pulay, in *Modern Theoretical Chemistry*, edited by H. F. Schaeffer III (Plenum, New York, 1977), Vol. 4, p. 153; *Mol. Phys.* **17**, 197 (1969).
- ⁴¹M. J. Sangster, G. Peckham, and D. H. Saunderson, *J. Phys. C* **3**, 1026 (1970).
- ⁴²See W. Kress, F. W. de Wette, A. D. Kulkarni, and U. Schröder, *Phys. Rev. B* **35**, 5783 (1987).
- ⁴³Ye Li, Ph.D. thesis, Rutgers University, 1994.